THE ASTROPHYSICAL JOURNAL, 562:649–653, 2001 December 1

POLARIZATION VLBI OBSERVATIONS OF THE GRAVITATIONAL LENS SYSTEM B0218+357 AT 8.4 GHz

A. J. KEMBALL
National Radio Astronomy Observatory, P.O. Box O, Socorro, NM 87801

AND

A. R. PATNAIK AND R. W. PORCAS
Max-Planck-Institut für Radioastronomie, Auf dem Hügel 69, D-53121, Bonn, Germany
Received 2001 June 8; accepted 2001 August 2

ABSTRACT

We present polarization VLBI observations of the gravitational lens system B0218+357 at an observing frequency of 8.4 GHz. The lensed components A and B show a core-jet substructure at milliarcsecond (mas) resolution, consistent with the quantitative lensing properties known for the system. The identified core is linearly polarized at a level of 8%–12%. The polarization position angle difference between A and B is consistent with the expected behavior of polarized emission under gravitational lensing and the known rotation due to differential Faraday rotation along the two lines of sight through the lensing galaxy. The mas polarization structure confirms the expected parity reversal for the two lensed components predicted by generic lens models for this system. Indirect evidence is presented in support of the BL Lacertae optical classification of the lensed object.

Subject headings: BL Lacertae objects: individual (0218+357) — galaxies: jets — gravitational lensing — polarization

1. INTRODUCTION

The cosmological importance of radio-interferometric studies of gravitational lenses is well established, both through the identification of multiply imaged lens systems and, where a lensing model is known, through the promise such observations hold for determining the Hubble constant H_0 by measuring the time delay of the lens (Refsdal 1964). Very long baseline interferometric (VLBI) observations sensitive to linearly polarized emission offer important new insights by allowing the radio polarization structure of gravitational lenses to be determined at milliarcsecond (mas) resolution, as demonstrated for the lens system B1422+231 by Patnaik et al. (1999). Such observations can confirm gravitational lens candidates through the expected invariance of polarization properties under gravitational lensing (Dyer & Shaver 1992) after taking account of Faraday rotation in the intervening lensing medium. They also provide information on the fine-scale polarization structure needed to interpret monitoring observations at lower spatial resolution using connected-element telescopes. Polarization VLBI monitoring is a more sensitive indicator of intrinsic source evolution, such as the emergence of new components near the core of a compact radio source. In addition, the milliarcsecond polarization structure provides new constraints on the lens magnification properties.

In this paper we present 8.4 GHz polarization VLBI observations of the gravitational lens system B0218+357. This source currently has the smallest known angular separation for a gravitational lens system and is an excellent candidate for the determination of H_0. The source was first proposed as a gravitational lens by Patnaik et al. (1992) and formed part of a Very Large Array (VLA) survey of candidate gravitational lenses selected from the Green Bank point source catalogs (Condon, Broderick, & Seielstad 1989). The radio structure as determined by VLA and MERLIN imaging includes an Einstein ring (O'Dea et al. 1992; Patnaik et al. 1993; Biggs et al. 2001) of diameter ~ 335 mas and has two flat-spectrum point components located northeast and southwest of the ring center (hereafter B and A, respectively). The ring emission has a steep spectrum ($\alpha \sim -0.6$) and is significantly polarized (O'Dea et al. 1992; Patnaik et al. 1993). VLA observations at 8.4 GHz show that the compact components A and B have a flux density ratio A/B = 3.24 and that both components are significantly polarized at $\sim$6%–8% (Patnaik et al. 1993). VLA monitoring at this frequency by Biggs et al. (1999) implies a flux density ratio of $\sim$3.5. The differential rotation measure between these two component has been measured to be ~ 910 rad m^{-2} (Patnaik et al. 1993).

The redshift of the lensing galaxy has been measured using optical spectroscopy (Browne et al. 1993) and confirmed by absorption detected toward B0218+357 in several radio molecular and atomic lines. These include H I (Carilli, Rupen, & Yanny 1993; Carilli et al. 2000), H_2CO (2_{11}–2_{12}) (Menten & Reid 1996), CO (1–2), CO (2–3), HCO^+ (1–2), HCN (1–2) (Wiklind & Combes 1995), ^{13}CO (4–3) (Gerin et al. 1997), ortho-H_2O (Combes & Wiklind 1997), and tentatively LiH (Combes & Wiklind 1998), all of which are consistent with a redshift for the lensing galaxy of 0.6847. The lensing galaxy has measured optical colors consistent with a spiral galaxy (Keeton, Kochanek, & Falco 1998). Optical spectroscopy has detected Mg II emission lines from the lensed object (Lawrence 1996; Browne et al. 1993), yielding a redshift estimate of 0.96. The optical classification of the lensed object is uncertain, but a BL Lacertae classification has been proposed based on the red, relatively featureless optical spectrum (Stickel & Kühr 1993). Optical imaging of the B0218+357 lensing system using the *Hubble Space Telescope* has been reported by Jackson, Xanthopoulos, & Browne (2000) and Lehár et al. (2000).

Total-intensity 15 GHz VLBI observations by Patnaik, Porcas, & Browne (1995) confirm the established lensing hypothesis for this object and reveal a core-jet structure for

the lensed components on the mas scale. A time delay $\tau = 10.5 \pm 0.4$ days has been reported for the system based on intensive VLA monitoring of variability in the total and linearly polarized intensity of the two components (Corbett et al. 1996; Biggs et al. 1999; Cohen et al. 2000). Combined with systematic efforts to model the lens system (Nair 1996), this source holds significant promise in the quest to measure the Hubble constant.

We discuss the mas polarization VLBI images presented here in terms of the lens hypothesis and magnification properties for this system, the relationship to connected-element polarization monitoring, and implications for the optical classification of the lensed object. The technical aspects of the observations and data reduction are discussed in § 2 and the results and discussion are presented in § 3.

2. OBSERVATIONS AND DATA REDUCTION

The data were taken in a 12 hr observing run starting at 1200 UT on 1995 May 9. All 10 antennas of the Very Long Baseline Array[1] (VLBA) were used, in conjunction with the phased VLA (in D configuration) and the 100 m Effelsberg telescope. The antenna characteristics for this network are listed in Table 1. The sources 3C 84 and 0234+285 were included in the observing session as polarization calibrators. Dual circular polarization was recorded at each antenna with a bandwidth of 32 MHz per polarization, spanned by two baseband converters recording upper and lower sidebands of 8 MHz each. The lower edge frequency of the recorded 32 MHz band in each polarization was 8.39949 GHz. The data were recorded in VLBA format using 1 bit quantization and correlated in full cross-polarization at the VLBA correlator in Socorro, New Mexico. The data were correlated in a single pass using a field center position of $\alpha(\mathrm{J2000}) = 02^{\mathrm{h}}21^{\mathrm{m}}05\overset{\mathrm{s}}{.}483$, $\delta(\mathrm{J2000}) = 35°56'13\overset{''}{.}78$ and a correlator accumulation period of 2.1 s, which was sufficient to meet the wide-field imaging requirements for this lens system. The nominal correlator frequency resolution was 0.5 MHz. The geometric mean of the synthesized array beamwidth using natural weighting was 1.3 mas.

The data were reduced using the AIPS and AIPS++ data reduction packages, applying methods described by Cotton (1993), Kemball, Diamond, & Pauliny-Toth (1996), and Patnaik et al. (1999). A brief synopsis of the data reduction process is given here. The data were corrected for known correlator effects and amplitude gain factors applied from a priori amplitude calibration information, comprising system temperature and recent gain curve information for the VLBA and the Effelsberg telescope and the measured ratio of antenna temperature to system temperature at the phased VLA. The flux densities of the observed sources were determined using the simultaneous 50 MHz connected-element data taken at the VLA, relative to the known flux densities for 3C 48 and 3C 138. The data were edited using on-line monitor data and station log information and by interactive and automated techniques. Cross-power bandpass corrections, modeled as complex polynomial expansions in amplitude and phase, were derived from the observed calibrator data and normalized to unit mean amplitude. The parallel-hand data (RR and LL) were fringe-fit for both residual delay and fringe-rate using global methods described by Schwab & Cotton (1983). The RL delay and phase offsets at the reference antenna, assumed to be time-invariant, were determined using averaged cross-polarized calibrator data.

All calibrator sources were imaged in Stokes I using standard hybrid mapping techniques. Final amplitude corrections for B0218+357 were derived from smoothed amplitude self-calibration solutions obtained for the calibrator 0234+285. The source B0218+357 was then imaged in two subfields centered on components A and B using multifield CLEAN deconvolution (Schwab 1984) alternating with phase-only self-calibration. Several cycles of full fringe-fitting and hybrid mapping were completed iteratively for B0218+357 using a successively refined source model in each fringe-fitting step to ensure a common delay and fringe-rate center for the widely separated image subfields. All final images were made using natural weighting.

Instrumental feed contamination terms, also referred to as D-terms (Conway & Kronberg 1969), which reflect the deviation of the feed response from the nominal sense of circular polarization, were determined for both polarization calibrators 3C 84 and 0234+285 independently using several feed calibration algorithms. Feed calibration was derived from the 3C 84 data assuming zero linear polarization. For 0234+285 an iterative form of the similarity approximation was used (Cotton 1993), as well as a non-iterative coupled solution (Leppänen, Zensus, & Diamond 1995). For each polarization calibration method, separate D-terms were determined for each 8 MHz band to minimize the effect of possible frequency dependence in the instrumental polarization of the phased VLA. Errors in the derived polarization properties were determined by comparing the polarization images obtained for B0218+357 using all independent polarization calibration methods. The absolute RL phase difference at the reference antenna, or equivalently the absolute polarization position angle, was determined relative to the simultaneous connected-element VLA data, tied to an assumed absolute polarization position angle for 3C 138 of $-13\overset{\circ}{.}87$.[2]

3. RESULTS AND DISCUSSION

The 8.4 GHz VLBI maps obtained from these observations are shown in Figure 1, where Stokes I intensity is shown as a contour plot with an overlay of line vectors plotted parallel to the incident electric field direction, with length proportional to the linearly polarized intensity $P = (Q^2 + U^2)^{1/2}$. A summary of measured component

[1] The National Radio Astronomy Observatory (NRAO) is operated by Associated Universities, Inc., under cooperative agreement with the National Science Foundation.

TABLE 1

ANTENNA PARAMETERS

Station	Diameter	Nominal SEFD[a] (Jy)
VLBA	10 × 25 m	10 × 325
Effelsberg	100 m	45
Phased VLA.....	27 × 25 m	20

[a] System equivalent flux density.

[2] See the University of Michigan Radio Astronomy Observatory Database (1995), http://www.astro.lsa.umich.edu/obs/radiotel/umrao.html.

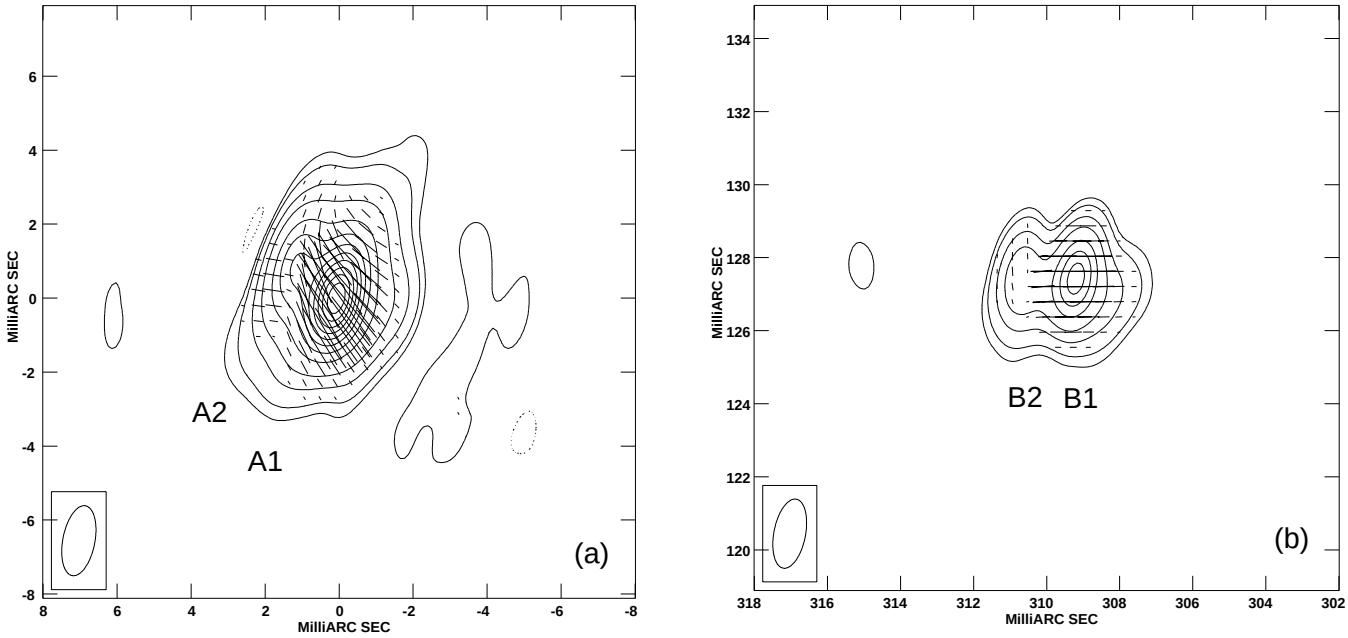

FIG. 1.—VLBI polarization map of B0218+357 at 8.4 GHz for (*a*) component A and (*b*) component B. Stokes *I* is plotted as a contour map with levels of 2.75 mJy beam^{-1} times (-10, -5, -2, -1, 1, 2, 5, 10, 20, 30, 40, 50, 60, 70, 80, 90, 100). The vectors indicate the plane of the electric field vector and have a length proportional to the linearly polarized intensity, where 1 mas = 12.8 mJy beam^{-1}.

TABLE 2

COMPONENT PROPERTIES

Component	Flux Density (mJy)	θ_{maj} (mas)	θ_{min} (mas)	p.a. (deg)	m_l (%)	χ (deg)
A1	544 ± 25	1.90 ± 0.3	1.12 ± 0.3	157 ± 6	8.0 ± 0.4	35.8 ± 1.5
A2	223 ± 5	≥ 2.0	≥ 2.0	...	...	...
B1	171 ± 5	0.72 ± 0.3	0.35 ± 0.04	73.2 ± 12.1	11.6 ± 0.4	90.3 ± 1.5
B2	59.9 ± 3	≥ 0.73	≥ 0.73	...	...	...

properties, as derived from the images shown in Figure 1, is given in Tables 2 and 3. The tabulated flux densities were measured by summing the flux density within polygon regions enclosing each component. This approach was taken to minimize systematic errors arising from the non-Gaussian shapes of the image components. Component positions and deconvolved sizes were estimated by fitting elliptical Gaussian components in the image plane. Uncertainties in the component size and position were conservatively estimated from the differences between images formed with uniform and natural weighting. Errors in the linear polarization properties were derived from different *D*-term calibrations and the overall uncertainty in the RL phase difference.

The overall morphology of the total intensity emission in Figure 1 follows closely that seen in earlier 15 GHz VLBI observations (Patnaik, Porcas, & Browne 1995), and is consistent with the established lensing hypothesis for this object. The individual components are distorted due to the lensing, including the tangential stretching expected at the position of component A for this system (Patnaik, Porcas, & Browne 1995). We adopt the same nomenclature as Patnaik, Porcas, & Browne (1995) with components A1, A2, B1, and B2 as indicated. The two VLBI components in each subfield (A or B) are interpreted as the inner jet of the lensed radio source, with (A1, B1) identified as the core. This identification is made on the grounds of the compactness of (A1, B1) with respect to (A2, B2) (Patnaik, Porcas, & Browne 1995), and the higher turnover frequency in the radio spectrum (Patnaik & Porcas 1999). The A1–B1 separation reported here agrees with that obtained in the 15 GHz VLBI observations, indicating that the same basic radio components are being observed at the two frequencies. Images made of a larger field than shown in Figure 1 did not detect the Einstein ring or any other compact components above a point source flux density limit of ~ 0.5 mJy. The nondetection of the Einstein ring is not unexpected for VLBI observations at 8.4 GHz, given the low peak surface brightness of this feature as measured in MERLIN observations.

TABLE 3

COMPONENT SEPARATIONS

Vector	Length (mas)	p.a. (deg)
A1–A2.....	1.47 ± 0.04	53.5 ± 2.5
B1–B2	1.50 ± 0.05	92.3 ± 0.6
A1–B1	334.19 ± 0.06	67.61 ± 0.02

The flux density ratios between corresponding components in each subfield are measured here to be A1/B1 = 3.2 ± 0.2 and A2/B2 = 3.7 ± 0.2. This compares well with reported VLA flux density ratios between the A and B fields of 3.24 (Patnaik et al. 1993) and ~ 3.5 (Biggs et al. 1999), although our values are uncorrected for the source

variability on timescales shorter than the image time-delay. At 15 GHz, Patnaik, Porcas, & Browne (1995) report component separations A1–A2 of 1.38 mas in p.a. $+51^\circ$ and B1–B2 of 1.47 mas in p.a. $+90^\circ$). Our 8.4 GHz separation values differ from these but have the expected orientation. Such differences in the component separations may, however, be explained by a frequency-dependent shift in the peak of the core or jet components. There is no strong information on the time evolution of the intrinsic component positions at mas resolution.

The observations presented here are the first to show the polarization structure of B0218+357 on a mas scale, and reveal that the dominant source of polarized emission is the component identified as the core (A1, B1). As visible in Figure 1, we find weak linearly polarized emission near components (A2, B2) at a level of less than one-tenth of the integrated linearly polarized emission of (A1, B1) and offset from the (A2, B2) peak component position in Stokes *I*. We designate these components A2P and B2P, located east and northeast of components A1 and B1, respectively. An even weaker polarized component is visible to the north of A2, but we do not detect an obvious counterpart in field B for this component, most likely due to sensitivity limitations or insufficient spatial resolution.

The differential polarization position angle between A1 and B1 is measured to be $54^\circ.5 \pm 1^\circ.5$. Assuming a λ^2 law with zero intercept for the differential Faraday rotation in the intervening lensing galaxy and no π ambiguities, this implies a rotation measure estimate of 747 ± 21 rad m^{-2}. Patnaik et al. (1993) report a rotation measure of 910 rad m^{-2} from VLA observations. The difference may reflect the different spatial scales sampled by the VLA and VLBI observations but could in principle be affected by intrinsic source variability on time scales shorter than the measured time delay for the system. The source is known to be variable in polarization position angle (Biggs et al. 1999). It is noted that at the redshift of the lensing galaxy, 1 mas = 3.9 h^{-1} pc, assuming $q_0 = 0.5$ and $h = H_0/100$ km s^{-1} Mpc^{-1}.

The peak fractional polarization of components A1 and B1 (measured at the position of maximum Stokes *I*) is listed in Table 2. The fractional linear polarization of A1 and B1 is higher than measured values from 8.4 GHz VLA observations (Patnaik et al. 1993; Biggs et al. 1999). Component A is known to be progressively depolarized at frequencies of 15 GHz and below when measured with connected-element interferometers (Patnaik et al. 1993; Biggs et al. 1999). These observations show that this result carries over to observations at VLBI resolution.

As stated above, the total-intensity morphology shown in Figure 1 is consistent with the classification of this system as a gravitational lens. However, the mas polarization properties provide unique confirming evidence that components (A1, B1) and (A2, B2) are gravitationally lensed counterparts. The rough agreement in fractional linear polarization and mas polarization structure are important points in this regard, despite the fact that exact agreement is not expected due to the known depolarization of A relative to B noted above. The polarization position angle data are consistent with the expectation that gravitational lensing does not rotate the position angle of linearly polarized emission (Dyer & Shaver 1992) after removing the known Faraday rotation in the intervening lensing galaxy of this system. In addition, the differential magnification matrix derived from the 15 GHz VLBI observations (Patnaik, Porcas, & Browne 1995), when applied to the measured 8.4 GHz vector separation of B1 and B2, predicts a separation vector between A1 and A2 of 1.49 mas at a position angle of $41^\circ.6$, in modest agreement with the measured result given in Table 3 and in keeping with the expected achromatic property of gravitational lensing. In addition, we note that components A2P and B2P are located on opposite sides of the axes (A1–A2, B1–B2) consistent with the parity reversal predicted by generic lens models for this system (Patnaik, Porcas, & Browne 1995). As visible in Figure 1, there is a locus of zero linear polarization between A1–A2P and B1–B2P in accord with the significant rotation in electric vector position angle apparent between components 1 and 2. The measured vectors (A1–A2P, B1–B2P) are biased from their true values by the close separation of the oppositely polarized components. The 15 GHz VLBI differential magnification matrix predicts (A1–A2P) of 2.4 mas at a position angle of 95°, against a measured value of 1.8 mas at a position angle of 82°, which is broadly consistent given the uncertainties in the true vectors (A1–A2P, B1–B2P) noted above. The differential magnification matrix should be fully determined by the measured vectors (B1–B2, B1–B2P) and their transformed counterparts (A1–A2, A1–A2P). We derived a differential magnification matrix in this manner but the resulting determinant is lower than the known flux density ratio A1/B1 for the system, and we do not report the matrix here. We believe that this determination of the magnification matrix was adversely affected by the systematic errors in estimating (A1–A2P, B1–B2P) discussed above. This issue will be resolved by future polarization VLBI studies at higher frequencies and correspondingly higher spatial resolution.

The mas polarization structure can also be used to provide supplementary information regarding the optical classification of the lensed object. The source has been classified as a BL Lac object on the basis of the red, featureless optical spectrum (Stickel & Kühr 1993). The high radio polarization of $\sim$8%–12% measured for the core in these observations favors a BL Lac classification over classification as a quasar, based on the statistical radio polarization properties of these two classes of sources as determined by polarization VLBI surveys at centimeter wavelengths (Cawthorne et al. 1993). Quasars typically have core polarizations that do not exceed 2% at centimeter wavelengths (Cawthorne et al. 1993), while BL Lac objects are more highly polarized (Gabuzda et al. 1992). The core polarization of B0218+357 is anomalously high even for a BL Lac classification, however, and the absence of polarization in the identified jet component is difficult to explain in terms of standard polarization models for radio jets without invoking external depolarization at a point along the line of sight between the source and the lensing galaxy. Higher fractional polarization may result if the lens magnifies a smaller, highly polarized region of the inner jet, thus minimizing the blending of polarized subcomponents. The differential magnification factor of $\sim$3.5, taken together with the lens geometry, argues against this interpretation, however, and also does not support high magnification gradients at the position of component A. The source is known to be variable in polarization (Corbett et al. 1996; Biggs et al. 1999), and VLBI monitoring will provide further insight regarding this question. Less conclusively, the lensing geometry suggests that the unlensed position angle of the projected jet axis must be intermediate between the position angles of

A1–A2 and B1–B2, i.e. $\sim 50°$–$90°$. For moderate Faraday rotation along the line of sight to A, the electric vector of the polarized emission is closer to parallel than to perpendicular to the jet axis, thus favoring a BL Lac classification (Gabuzda et al. 1992). It is noted that the lens system 1938+666 has a similarly anomalously high component polarization of $\sim 15\%$ (King et al. 1997). The higher redshift of gravitationally lensed objects implies a higher frequency in the source rest frame, which may be partly responsible for the increased fractional polarization observed in these systems. This effect for B0218+357, however, with a source redshift of 0.96, is modest.

These VLBI observations are also of relevance to radio monitoring campaigns to determine the time delay for this gravitational lens system. By identifying the dominant polarized component as the core, these observations strengthen the basis of the time-delay measurements derived using the VLA (Biggs et al. 1999), which implicitly assume a single, predominant compact polarized component in each subfield.

We would like to thank the operations staff at the Effelsberg and VLBA antennas and the correlator group in Socorro for their support with these observations. These were among the first Effelsberg observations recorded in VLBA format and we thank Dr. D. Graham of the MPIR for his technical assistance in this regard. This research has made use of data from the University of Michigan Radio Astronomy Observatory, which is supported by funds from the University of Michigan. We would like to thank the referee for helpful comments.

REFERENCES

Biggs, A. D., Browne, I. W. A., Helbig, P., Koopmans, L. V. E., Wilkinson, P. N., & Perley, R. A. 1999, MNRAS, 304, 349
Biggs, A. D., Browne, I. W. A, Muxlow, T. W. B., & Wilkinson, P. N. 2001, MNRAS, 322, 821
Browne, I. W. A., Patnaik, A. R., Walsh, D., & Wilkinson, P. N. 1993, MNRAS, 263, L32
Carilli, C. L., Rupen, M. P., & Yanny, B. 1993, ApJ, 412, L59
Carilli, C. L., et al. 2000, Phys. Rev. Lett., 85, 5511
Cawthorne, T. V., Wardle, J. F. C., Roberts, D. H., & Gabuzda, D. C. 1993, ApJ, 416, 519
Cohen, A. S., Hewitt, J. N., Moore, C. B., & Haarsma, D. B. 2000, ApJ, 545, 578
Combes, F., & Wiklind, T. 1997, ApJ, 486, L79
———. 1998, A&A, 334, L81
Condon, J. J., Broderick, J. J., & Seielstad, G. A. 1989, AJ, 97, 1064
Conway, R. G., & Kronberg, P. P. 1969, MNRAS, 142, 11
Corbett, E. A., Browne, I. W. A., Wilkinson, P. N., & Patnaik, A. R. 1996, in Astrophysical Applications of Gravitational Lensing, ed. C. S. Kochanek & J. N. Hewitt (Dordrecht: Kluwer), 37
Cotton, W. D. 1993, AJ, 106, 1241
Dyer, C. C., & Shaver, E. G. 1992, ApJ, 390, L5
Gabuzda, D. C., Cawthorne, T. V., Roberts, D. H., & Wardle, J. F. C 1992, ApJ, 388, 40
Gerin, M., Phillips, T. G., Benford, D. J., Young, K. H., Menten, K. M., & Frye, B. 1997, ApJ, 488, L31
Jackson, N., Xanthopoulos, E., & Browne, I. W. A. 2000, MNRAS, 311, 389
Keeton, C. R., Kochanek, C. S., & Falco, E. E. 1998, ApJ, 509, 561
Kemball, A. J., Diamond, P. J., & Pauliny-Toth, I. I. K. 1996, ApJ, 464, L55
King, L. J., Browne, I. W. A., Muxlow, T. W. B., Narasimha, D., Patnaik, A. R., Porcas, R. W., & Wilkinson, P. N. 1997, MNRAS, 289, 450
Lawrence, C. R. 1996, in Astrophysical Applications of Gravitational Lensing, ed. C. S. Kochanek & J. N. Hewitt (Dordrecht: Kluwer), 299
Lehár, J., Falco, E. E., Kochanek, C. S., McLeod, B. A., Munoz, J. A., Impey, C. D., Rix, H.-W., Keeton, C. R., & Peng, C. Y. 2000, ApJ, 536, 584
Leppänen, K. J., Zensus, J. A., & Diamond, P. J. 1995, AJ, 110, 2479
Menten, K. M., & Reid, M. J. 1996, ApJ, 465, L99
Nair, S. 1996, in Astrophysical Applications of Gravitational Lensing, ed. C. S. Kochanek & J. N. Hewitt (Dordrecht: Kluwer), 197
O'Dea, C. P., Baum, S. A., Stanghellini, C., Dey, A., van Breugel, W., Deustua, S., & Smith, E. P. 1992, AJ, 104, 1320
Patnaik, A. R., Browne, I. W. A., King, L. J., Muxlow, T. W. B., Walsh, D. W., & Wilkinson, P. N. 1992, in Gravitational Lenses, ed. R. Kayser, T. Schramm, & L. Nieser (Berlin: Springer), 140
———. 1993, MNRAS, 261, 435
Patnaik, A. R., Kemball, A. J., Porcas, R. W., & Garrett, M. A. 1999, MNRAS, 307, L1
Patnaik, A. R., & Porcas, R. W. 1999, in ASP Conf. Ser. 156, Highly Redshifted Radio Lines, ed. C. L. Carilli, S. J. E. Radford, K. M. Menten, & G. I. Langston (San Francisco: ASP), 247
Patnaik, A. R., Porcas, R. W., & Browne, I. W. A. 1995, MNRAS, 274, L5
Refsdal, S. 1964, MNRAS, 128, 307
Schwab, F. R. 1984, AJ, 89, 1076
Schwab, F. R., & Cotton, W. D. 1983, AJ, 88, 688
Stickel, M., & Kühr, H. 1993, A&AS, 101, 521
Wiklind, T., & Combes, F. 1995, A&A, 299, 382